

## 4/3 Law of Granular Particles Flowing through a Vertical Pipe

Osamu Moriyama, Naoya Kuroiwa, and Mitsugu Matsushita

*Department of Physics, Chuo University, Kasuga, Bunkyo-ku, Tokyo 112-8551, Japan*

Hisao Hayakawa

*Graduate School of Human and Environmental Studies, Kyoto University, Sakyo-ku, Kyoto 606-8501, Japan*

(Received 16 June 1997)

Density waves of granular material (sand) flowing through a vertical pipe have been investigated. Clear density waves emerge when the cock attached to the bottom end of the pipe is closed. The FFT power spectra were found to show a stable power-law form  $P(f) \sim f^{-\alpha}$ . The value of the exponent was evaluated as  $\alpha \cong 4/3$ . We also introduce a simple one-dimensional model which reproduces  $\alpha = 4/3$  from both simulation and theoretical analysis. [S0031-9007(98)05707-X]

PACS numbers: 46.10.+z, 05.20.Dd, 05.70.Jk, 81.05.Rm

Recently much attention has been paid to the dynamics and statistics of granular materials because of their ubiquity in nature and the application to technology. Unlike usual solids, liquids, or gases, granular materials are known to show complex dynamical behaviors [1], such as convection [2], size segregation [3], bubbling [4], standing waves and localized excitations under vertical vibration [5,6], and a fluidized bed due to air injected inside a box containing granules [7,8].

Pattern formation of grains flowing through a vertical pipe which can be regarded as a one-dimensional realization of a fluidized bed is also a typical example of unusual features of granular motion [9–13]. Emergence of density waves (e.g., slugging) has been investigated by molecular dynamics (MD) and lattice-gas automata (LGA) simulations [9,10] and by the experiments using sand in air [11,12] and metallic spheres in liquids [13]. The power-law form of the power spectrum  $P(f) \sim f^{-\alpha}$ , where  $f$  is frequency, of density fluctuations was also found in both numerical simulations [9] and experiments [11,12]. Although their interpretations on the origin of the emergence of density waves are different, estimated values of the exponent  $\alpha$  are close to each other ( $1.3 < \alpha < 1.5$ ).

Although the previous experiment [11,12] reported  $\alpha \cong 1.5$ , some of their experimental procedures seem a little ambiguous: Since they merely plugged up the bottom hole of a pipe by half in order to induce density waves, the rate of air flow out of the bottom end of the pipe was not well controlled. Besides, the power spectra they obtained were still noisy. In this Letter we will first present better-controlled air flow out of the pipe and more accurate experimental results than the previous ones by increasing the number of trials. One of our results is the precise estimation of the scaling exponent of the power spectrum  $P(f) \sim f^{-\alpha}$ . The result is  $\alpha \cong 4/3$ . We also propose a one-dimensional model supplemented by the white noise which reproduces  $\alpha = 4/3$  near the neutral curve of the linear stability analysis of uniform states. In other words, we will clarify the origin of the power law in density waves of granular pipe flows.

Our experimental setup is shown in Fig. 1. We used a glass pipe of 1500 mm length and 3 mm inner diameter, i.e., the same one used in Refs. [11,12]. A flask is connected to the bottom end of the vertical pipe, and a flow meter is attached to an outlet stuck out of the flask. We used rough sand; i.e., our granular particles are polydisperse, and their average diameter is about 0.3 mm. Thus the inner diameter of the pipe is about 10 times larger than the average diameter of sand. We pored rough sand into a hopper connected to the top end of the pipe, which flows through the pipe due to gravity. Sand finally falls into the flask, while air can exit out of it through the flow meter, which can control the rate of air discharge. Meanwhile, we measured density fluctuations as the transmission light intensity across the pipe at a fixed location midway up the pipe by using laser light and detecting system (KEYENCE, LX2-02). The laser light has a rectangular cross section of 10 mm wide and 1 mm high and is emitted with a pulse frequency of 4096 Hz. The detecting system has linear response between the output voltage and the density of particles in the range of output voltage between 1 and 5 V.

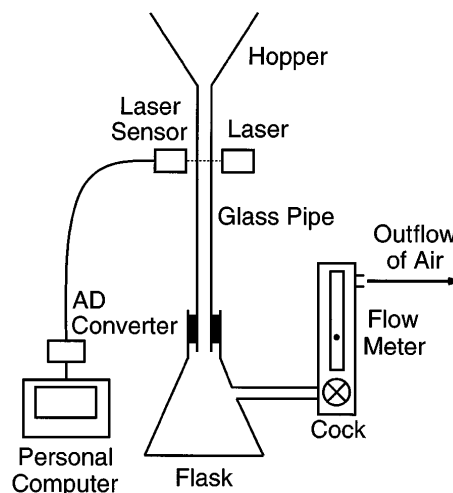


FIG. 1. Schematic illustration of the experimental setup.

Let us now consider what happens by closing the cock of the flow meter. Granular particles falling in a pipe interact with the medium (air) due to the viscosity. When the flow meter is removed from the apparatus, i.e., the bottom end of the pipe is fully open, granules can fall rather freely as if the existence of air could be neglected. (Hereafter we will refer to this situation as *fully open*.) In fully open there are no visible density waves, as reported in Refs. [11,12]. The reason is that both granules and air flow together through the pipe. As the cock is gradually closed, however, the pressure in the flask rises, and the effect of the viscous force becomes more important. In particular, when the cock is fully closed (we refer to *fully closed*), air in the pipe must go upward due to approximate conservation of the total volume (sand plus air) in the flask while sand falls downward. We consider that the increment of interaction between granules and air induces density waves.

Figure 2 shows typical time series signals of granular flows measured at  $x = 100$  cm, where  $x$  is defined as the distance of measuring point along the pipe from the top. In contrast with the white-noise-like signal (top) in fully open, one can see that the density wave for fully closed (bottom) has intermittent structure. In this figure higher (lower) voltage corresponds to smaller (larger) granular density since we measured the light intensity transmitted across the pipe. In particular, the output voltage is about 2.15 V when a pipe is fully packed with sand, and about 2.50 V when it is completely empty. This assures us that our measurements were well in the linear range between the voltage and the density. In the case of real flow patterns one can observe that two clusters sometimes collide with each other and merge into

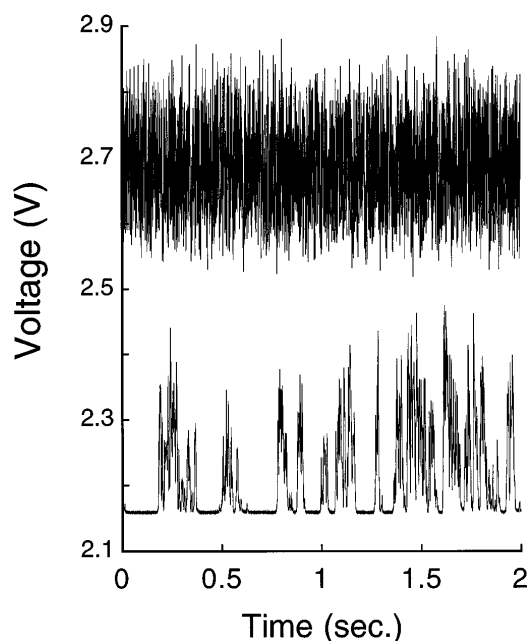


FIG. 2. Time series signal of the granular flows for *fully open* (top) and *fully closed* (bottom). Upper signal is shifted by 0.4 V to avoid the data overlap.

one, and sometimes one cluster splits into more than one cluster, in a behavior reminiscent of a chain of traffic jams on a crowded highway [14–16]. In the following discussion of this Letter we restrict ourselves to fully closed. (When the medium air was controlled to flow downward by gradually opening the cock of the flow meter, the position of the emergence of clear density waves gradually shifted downward. The details of the results will be presented elsewhere.)

Let us pay attention to the power spectrum  $P(f)$  of density fluctuations of granular flows. Figure 3 shows  $P(f)$  of recorded signals in fully closed. Each spectrum was obtained by averaging over 640 independent data with length 8192 discrete points each (2 s in real time) and was appropriately shifted to avoid the overlap. The self-organization of the power-law form  $P(f) \sim f^{-\alpha}$  is observed as the measuring position  $x$  increases: The spectrum at  $x = 10$  cm is similar to that in fully open. Density waves have already emerged at  $x = 40$  cm where the scaling regime is covered by the whole frequency range except for the fast decay in higher  $f$ . Then the system falls into the steady state from about  $x = 50$  cm downward. The scaling range for the steady state, i.e., for  $x \geq 50$  cm is from 10 to 200 Hz, as seen in Fig. 3.

In the frequency range from 15 to 150 Hz, values of the slope are fitted by the least mean square method as  $\alpha = 1.33 \pm 0.04$ ,  $1.31 \pm 0.05$ , and  $1.34 \pm 0.05$  for  $x = 80, 90,$  and  $100$  cm, respectively. (The data at  $x = 90$  and  $100$  cm are not shown in Fig. 3.) These values are very close to  $4/3$  suggested by LGA simulation [9].

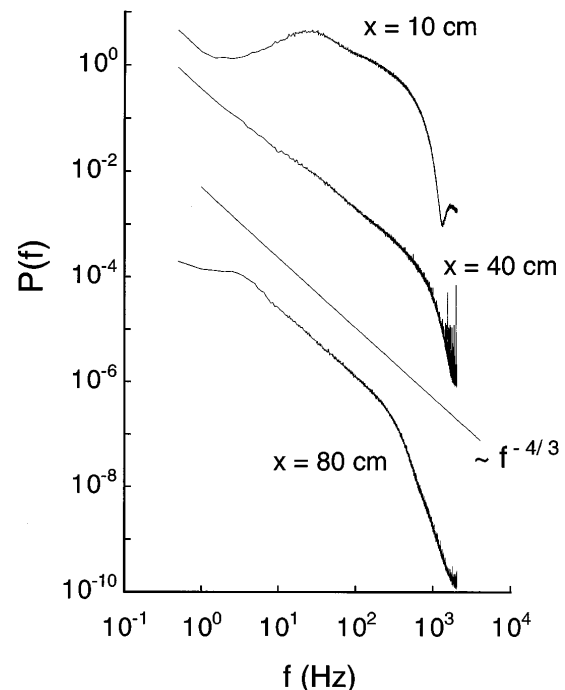


FIG. 3. Log-log plot of power spectra  $P(f)$  of time series signals in *fully closed*. The straight line with the slope of  $-4/3$  in the figure is a guide for the eyes.

Let us allocate the rest of this Letter to introduce a one-dimensional model which reproduces  $\alpha = 4/3$  in a fully closed system.

The important mechanisms for particle dynamics are the drag between air and particles, and the relaxation process to an optimal velocity which may be the sedimentation rate of particles. When the  $N$  particles are confined in a quasi-one-dimensional container, the motion of particles may be described by the following nonlinear equation:

$$\ddot{r}_n + \zeta[\dot{r}_n - W(\{r_n\})] = TF(\{r_n\}) + f_n(t), \quad (1)$$

where  $r_n$  and  $\zeta$  are the relative distance between the  $n$ th and  $(n+1)$ th particles, and the drag coefficient, respectively. The collisional force  $F(\{r_n\}) = \varphi'(r_{n+1}) + \varphi'(r_{n-1}) - 2\varphi'(r_n)$  comes from a soft core repulsive potential  $\varphi(r_n)$ . The parameter  $T$  represents the strength of repulsion. The optimal velocity  $W(\{r_n\}) = U(\frac{r_{n+1}+r_n}{2}) - U(\frac{r_n+r_{n-1}}{2})$  is the linear combination of sedimentation rate  $U(x)$  which is the nonlinear function of the local volume fraction [17] in general. The most crucial simplification of (1) without any justification is to assume that  $f_n$  is a Gaussian white noise with zero mean. It should be noticed that the drag  $\zeta$  is irrelevant in fully open, because air in the pipe flows away together with particles. Thus, the motion of particles is almost elastic, and clear density waves cannot be observed in fully open. It should be noted that (1) is written for the relative motion of particles. Discarding the noise term from (1), we obtain an equation of motion for the particle at the position  $x_n$  as  $\ddot{x}_n + \zeta[\dot{x}_n - U(\frac{x_{n+1}-x_{n-1}}{2})] = T[\varphi'(r_n) - \varphi'(r_{n-1})]$  where  $r_n = x_{n+1} - x_n$ .

Linearizing (1) around the uniform solution  $\dot{r}_n = 0$  where  $a = \bar{r}_n \equiv N^{-1} \sum_n r_n$ , we obtain

$$\ddot{\tilde{r}}_k + \zeta[\dot{\tilde{r}}_k - iU' \sin k \tilde{r}_k] = 2T\varphi''(\cos k - 1)\tilde{r}_k + \tilde{f}_k(t), \quad (2)$$

where the argument of  $U'$  and  $\varphi''$  is  $a$ .  $\tilde{r}_k$  and  $\tilde{f}_k(t)$  are, respectively, the Fourier transform of  $\delta r_n = r_n - a$  and  $f_n(t)$ . Equation (2) has the solution  $\tilde{r}_k(t) \propto \exp[\sigma_{\pm} t]$ , where

$$\sigma_{\pm} = -\frac{\zeta}{2} \pm \sqrt{\left(\frac{\zeta}{2}\right)^2 - 2T\varphi''(1 - \cos k) + i\zeta U' \sin k}. \quad (3)$$

$\text{Re}[\sigma_{+}]$  represents the relevant eigenvalue of the linear problem, which becomes positive for  $U'(a)^2 \cos^2(k/2) \geq T\varphi''(a)$ . Thus the most unstable wave number is  $k \rightarrow 0$ , and the neutral curve is given by  $T_c = U'^2/\varphi''(a)$ . At  $T = T_c(1 - \mu)$  the expansion of  $\sigma_{+}$  around  $k = 0$  is given by

$$\sigma_{+}(k) \simeq i\left[c_0 k - \frac{c_0}{6} k^3 + \dots\right] + \frac{c_0 \mu}{\zeta} k^2 - \frac{c_0^2}{4\zeta} k^4 + \dots,$$

where  $c_0 = U'(a)$ . Thus, for  $\mu > 0$  the uniform state is unstable due to the negative diffusion.

Adopting  $U(r) = \tanh(r-2) + \tanh(2)$ ,  $\varphi(r) = \text{sech}^2(r)$ ,  $\zeta = 2$ ,  $N = 256$ ,  $T_c = 3.95798\dots$ , and  $a = 2$  at  $t = 0$ , we simulated (1) by the classical Runge-Kutta method until  $t = 2^{11}$  with time interval  $\Delta t = 1/2^4$  under the periodic boundary condition. We used the uniform random number distributed between  $-X$  and  $X$  with  $X = 9/1024$  [18] for  $f_n(t)$ . Figure 4 displays the power spectrum  $P(f) = |\tilde{c}(f)|^2$  obtained from our simulation of (1) at  $\mu = 1/64$ , where  $\tilde{c}(f)$  is the Fourier transform of the discretely sampled data of the density  $c(t) = \frac{1}{N} \sum_n \frac{1}{r_n(t)}$  with the interval 1. This clearly supports  $P(f) \sim f^{-4/3}$  as in our experiment. From the examinations of several values of  $\mu$ , we have confirmed that the qualitative results are insensitive to the sign of  $\mu$  when  $|\mu| \ll 1$ . This result is reasonable because near the neutral curve the time scale of relaxation or growth of fluctuations is much longer than the time scale induced by the noise  $f_n(t)$ . Our result suggests that the linear relaxation theory of fluctuations can be used to explain  $P(f) \sim f^{-4/3}$ .

Let us briefly sketch how to derive the 4/3 law from the behavior of structure factor

$$S_k(t) = \sum_{n,m} \langle \exp\{ik[\delta r_n(t) - \delta r_m(0)]\} \rangle \quad (4)$$

in weakly stable states, i.e.,  $\mu < 0$  and  $|\mu| \ll 1$ , where  $\delta r_n = r_n - a$  is the fluctuation of relative distance. The structure factor can be rewritten as  $S_k(t) = \frac{1}{N} \sum_{n,m} \exp[-\frac{k^2}{2} \phi_{nm}(t)]$  where  $\phi_{nm}(t) = \langle [\delta r_n(t) - \delta r_m(0)]^2 \rangle$ . For  $\mu < 0$ ,  $S_k(t)$  can be calculated as in

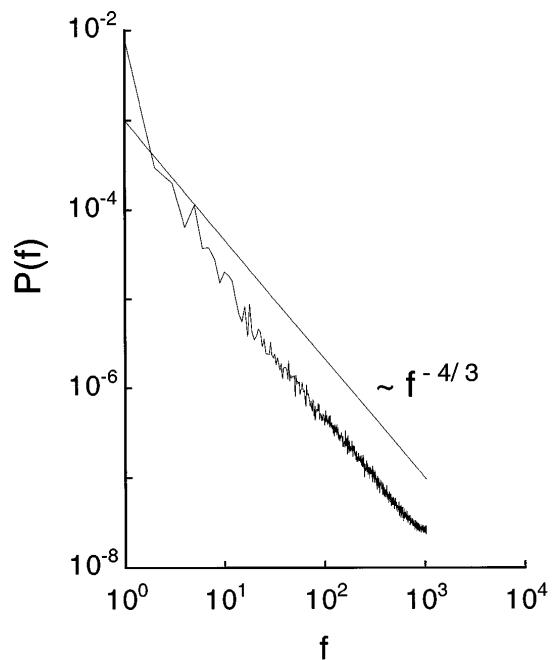


FIG. 4. Log-log plot of power spectrum  $P(f)$  obtained from the numerical integration of (1), where the unit of  $f$  is  $1/2\pi$ . The guide line represents  $f^{-4/3}$ . See the text for details.

the case of polymer dynamics [19]. With the aid of the expansion of  $\sigma_+$ , (1) is reduced to

$$\partial_\tau r(z, \tau) - \partial_z^3 r(z, \tau) = \epsilon [\partial_z^2 - \partial_z^4] r(z, \tau) + \xi(z, \tau), \quad (5)$$

where  $\tau = \epsilon^3 \beta t$ ,  $z = \frac{2\zeta}{3c_0} \epsilon (x + c_0 t)$ , and  $\xi(z, \tau) = \epsilon^3 \beta f_n(t)$  with  $\epsilon = \frac{3\sqrt{c_0}}{\zeta} \sqrt{-\mu}$  and  $\beta = \frac{4}{3\sqrt{c_0}}$ . The solution of (5) is given by  $\tilde{r}_k(\tau) \approx \int_0^\tau ds \exp[\lambda_k(\tau - s)] \times \tilde{\xi}_k(s)$ , where  $\lambda_k = ik^3 - \epsilon k^2(1 + k^2)$ . Thus, we obtain the correlation

$$\langle \tilde{r}_k(\tau) \tilde{r}_{-k}(0) \rangle = \frac{D}{2\epsilon l k^2 (1 + k^2)} \exp[\lambda_k \tau], \quad (6)$$

where  $l$  is the system size, and we used  $\langle \tilde{\xi}_k(\tau) \tilde{\xi}_p(\tau') \rangle = \frac{D}{l} \delta_{k+p,0} \delta(\tau - \tau')$ .

A long but straightforward calculation parallel to Ref. [19] yields

$$S_k(\tau) \approx \int_{-l}^l dx \times \exp \left[ -D_G k^2 \tau - \frac{Dk^2}{2\epsilon} w - \frac{Dk^2}{\pi\epsilon} \tau^{1/3} h(u) \right], \quad (7)$$

where the argument of  $S_k$  is replaced by the scaled time,  $D_G$  is the diffusion constant for the gravitational center in (5),  $u = x\tau^{-1/3}$ , and  $w = |z - z'|$ . Since  $h(u)$  converges to  $h(0) = \pi/\Gamma(1/3)$  as time goes on, we obtain

$$S_k(\tau) \approx \frac{4\epsilon}{Dk^2} \exp \left[ -\frac{Dk^2}{\epsilon\Gamma(1/3)} \tau^{1/3} \right] \quad (8)$$

in intermediate time range. In the limit of small  $\tau$ ,  $S_k(\tau) \propto 1 - \frac{Dk^2}{\epsilon\Gamma(1/3)} k^2 \tau^{1/3} + \dots$ . Thus its Fourier transform, giving the power spectrum  $P_k(f)$  obeys

$$P_k(f) \sim f^{-\alpha}, \quad \alpha = 4/3 \quad (\text{as } f \rightarrow \infty), \quad (9)$$

where use was made of  $\int_0^\infty dt e^{i2\pi ft} |t|^{1/3} \propto f^{-4/3}$ . The value  $4/3$  is identical to the one obtained by our experiments and numerical simulations [9]. Thus our model (1) reproduces  $\alpha = 4/3$ . It should be noted that the appearance of this power-law form in the original model (1) is only for  $f < \zeta$  since we eliminate the fast decaying mode  $\sigma_-$  in our analysis. This tendency is also observed as the higher-frequency cutoff in our experiment (see Fig. 3).

The  $4/3$  law is determined by short time behavior of the dynamics of density waves induced by the noise, which is essentially determined by the linear dispersion relation  $\lambda_k \sim ik^3$ . The details of our theoretical analysis including the effects of nonlinearity will be discussed elsewhere [20].

In this Letter we have confirmed  $\alpha = 4/3$  as the power-law exponent in the frequency spectrum of density correlation function from the experiment, the simulation, and the theory. We have also clarified the mechanism to yield the  $f^{-4/3}$  spectrum which is related to the critical slowing down of the density fluctuations. It should be

noticed that the continuous increase of  $\alpha$  in LGA [10] from  $\alpha = 0$  to 2 with the particle density is consistent with the  $4/3$  law and our picture, because the spectrum determined by the noise in the linearly stable uniform state far from the neutral curve should be white ( $\alpha = 0$ ), and the effective exponent of the power law becomes large when the exponential decay (i.e.,  $\alpha = 2$ ) in the off-critical region exists. There is, however, a discrepancy between our results and the one on experiments in liquids [13]. The reason for this difference should be clarified in the future.

O.M., N.K., and M.M. thank Y-h. Taguchi, T. Isoda, and A. Nakahara for stimulating discussions. H.H. thanks K. Ichiki, K. Nakanishi, and G. Peng for fruitful discussions. This work is partially supported by Grant-in-Aid for Science Research Fund from the Ministry of Education, Science and Culture (09740314).

- 
- [1] H. M. Jaeger, S. R. Nagel, and R. P. Behringer, *Rev. Mod. Phys.* **68**, 1259 (1996).
  - [2] Y-h. Taguchi, *Phys. Rev. Lett.* **69**, 1367 (1992); K. M. Aoki, T. Akiyama, Y. Maki, and T. Watanabe, *Phys. Rev. E* **54**, 874 (1996).
  - [3] A. Rosato, K. J. Strandburg, F. Prinz, and R. H. Swendsen, *Phys. Rev. Lett.* **58**, 1038 (1987).
  - [4] H. K. Pak and R. P. Behringer, *Nature (London)* **371**, 231 (1994).
  - [5] F. Melo, P. B. Umbanhowar, and H. L. Swinney, *Phys. Rev. Lett.* **75**, 3838 (1995).
  - [6] P. B. Umbanhowar, F. Melo, and H. L. Swinney, *Nature (London)* **382**, 793 (1996).
  - [7] G. K. Batchelor, *J. Fluid Mech.* **193**, 75 (1988).
  - [8] S. Sasa and H. Hayakawa, *Europhys. Lett.* **17**, 685 (1992); T. S. Komatsu and H. Hayakawa, *Phys. Lett. A* **183**, 56 (1993).
  - [9] G. Peng and H. J. Herrmann, *Phys. Rev. E* **49**, R1796 (1994).
  - [10] G. Peng and H. J. Herrmann, *Phys. Rev. E* **51**, 1745 (1995).
  - [11] S. Horikawa, A. Nakahara, T. Nakayama, and M. Matsushita, *J. Phys. Soc. Jpn.* **64**, 1870 (1995).
  - [12] S. Horikawa, T. Isoda, T. Nakayama, A. Nakahara, and M. Matsushita, *Physica (Amsterdam)* **233A**, 699 (1996).
  - [13] A. Nakahara and T. Isoda, *Phys. Rev. E* **55**, 4264 (1997).
  - [14] M. Bando, K. Hasebe, A. Nakayama, A. Shibata, and Y. Sugiyama, *Phys. Rev. E* **51**, 1035 (1995).
  - [15] B. S. Kerner and P. Konhauser, *Phys. Rev. E* **48**, 2335 (1993).
  - [16] T. S. Komatsu and S. Sasa, *Phys. Rev. E* **52**, 5574 (1995).
  - [17] H. Hayakawa and K. Ichiki, *Phys. Rev. E* **51**, R3815 (1995), and references therein.
  - [18] The value of  $X$  is chosen to have the unit amplitude in the form of Eq. (5).
  - [19] P. G. de Gennes, *Physics* **3**, 37 (1967); see also M. Doi and S. F. Edwards, *The Theory of Polymer Dynamics* (Clarendon, Oxford, 1986).
  - [20] Detailed calculation within the linear theory discussed here can be seen in H. Hayakawa and K. Nakanishi, *Prog. Theor. Phys. Suppl.* (to be published).